

A hydrographic time series station in the Wadden Sea (southern North Sea)

Rainer Reuter · Thomas H. Badewien ·
Alexander Bartholomä · Axel Braun · Andrea Lübben ·
Jürgen Rullkötter

Received: 6 February 2009 / Accepted: 24 March 2009
© Springer-Verlag 2009

Abstract In the tidal inlet between the East Frisian islands of Langeoog and Spiekeroog, southern North Sea, a time-series station was set up in autumn 2002 as part of the research programme *BioGeoChemistry of Tidal Flats* run by the University of Oldenburg. The purpose of the station is to provide continuous data on physical, biological and chemical parameters. In addition to instruments recording basic hydrographic and meteorological parameters, the time-series station is equipped with acoustic Doppler profilers for measuring surface waves and current profiles. Compact optical spectrometers are being used for spectral measurements of seawater transmission and for daylight reflectance. Additional sensors were installed for measuring oxygen, nutrients and methane in the seawater. The data shall help to quantify the flux of dissolved and suspended matter between the backbarrier tidal flat and the open sea and to characterise the material transformation in the tidal

flat area by biogeochemical processes over the tidal cycle. Due to its novel design, operation of the station is also possible during winter and under extreme weather conditions (gales, storm surges, and sea ice) when data sampling with conventional platforms such as research vessels, buoys, or smaller poles could not be performed in the past. In this way, time series of data are obtained, which include events that are most relevant to the evolution of this coastal area. The performance of the station and its equipment are presented with data covering 6 years of operation. Time series of air and water temperature as well as seawater salinity demonstrate the multiyear dynamics of these parameters in the East Frisian Wadden Sea. Hydrographic data collected under specific meteorological conditions such as gales and storm surges exemplify the all-weather capabilities of the station and its value for studying hydrographic processes in the Wadden Sea.

Keywords Tidal flats · Wadden Sea · Hydrographic station · Time-series measurements · Coastal zone processes · Hydrography · Meteorology

Responsible Editor: Jörg-Olaf Wolff

R. Reuter (✉) · T. H. Badewien · A. Braun · A. Lübben
Institute of Physics (IfP), Carl von Ossietzky Universität
Oldenburg,
26111 Oldenburg, Germany
e-mail: rainer.reuter@uni-oldenburg.de
URL: <http://www.uni-oldenburg.de/meeresphysik>

A. Bartholomä
Senckenberg am Meer,
26382 Wilhelmshaven, Germany

R. Reuter · J. Rullkötter
Institute of Chemistry and Biology of the Marine Environment
(ICBM), Carl von Ossietzky Universität Oldenburg,
26111 Oldenburg, Germany

1 Introduction

The Wadden Sea coast characterises the southern North Sea. Their morphodynamics (Ehlers 1988) and physical water-column dynamics (Postma 1982; Dyer 2000) and ecology (Reise 1985) have been a subject of extensive studies. However, the fundamental physical, chemical and biological interactions characterising the existence and dynamics of these coastal zones have not yet been subject of systematic investigations. To obtain a better understanding of these dynamic processes, the interdisciplinary

research programme *BioGeoChemistry of Tidal Flats* was established with the following goals:

- To investigate the budget of matter fluxes between tidal flats and open coastal waters and of matter transformation in the tidal flat water column and the sediments
- To understand the relevance of microbial activity for exchange processes between sediment and water column
- To understand the relevance of external factors that control the materials transport and transformation such as storms, spring tides and ice during extreme winter conditions
- To develop an integrated model, supported by experimental data for its validation, for a systematic understanding of the tidal flat dynamics.

The major study site is the East Frisian Wadden Sea, with a focus on the region of Spiekeroog island (Fig. 1). In former project studies, data were only collected during short-term ship cruises in the backbarrier tideways and in the adjacent coastal zone. The most relevant event-related processes affecting the tidal flats, such as storm and storm surges, were quite likely missed.

To consider such individual events and achieve a continuous data availability, a time-series station was set up in summer 2002 in the tidal inlet of Spiekeroog island, i.e. in a position between the backbarrier tidal flat and the open coastal waters where the tidal-driven water exchange is highest. In this paper, we report on the technical layout of the time series station *Wattenmeer* and on the experience of its performance during 6 years of operation. The quality of

instruments and methods are described, as are the approaches to overcome limitations, which became apparent during operational use of the station. We further present and discuss data sets obtained with the sensors installed at the station. They demonstrate the value of continuous hydrographic measurements in this region and also cover periods of storm tides and gales when hydrographic data were previously mostly unavailable.

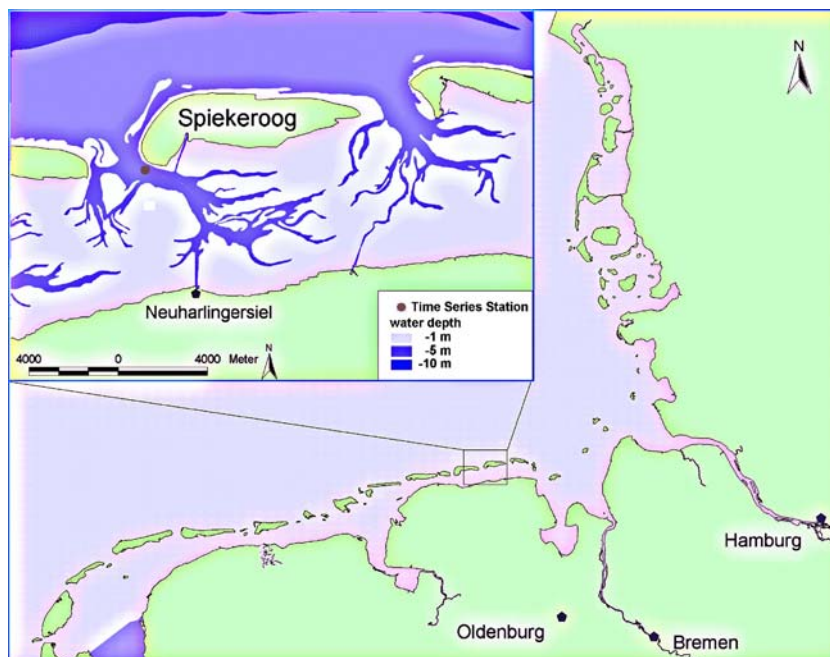
2 The station

2.1 Location and main features

The time-series station (Fig. 2) was erected in the tidal inlet between the islands of Langeoog and Spiekeroog at position 53°45'01.0" N, 007°40'16.3" E. The bottom depth at this location is 13 m below mean sea level (Normalnull NN). A summary of the technical layout is given in Table 1.

The station was designed for full-year operation, with a stability to withstand ice conditions of up to 50 cm ice thickness and wave heights, as they typically occur in that region under stormy weather conditions with northwesterly wind directions during winter. The mechanical structure consists of a pole having 35.5 m length and a diameter of 1.6 m, driven to 10 m depth into the sediment. On top of the pole is a platform about 7 m above the mean sea level, i.e. 3.6 m above mean high water springs, equipped with two laboratory containers. Above the containers is a second platform where a wind turbine and solar panels are installed for achieving an autonomous electrical power supply of the

Fig. 1 The area of interest, the tidal flats and catchment area near Spiekeroog island, southern North Sea. The position of the time-series station is marked with a red dot. Water depths given in blue colours refer to the mean sea level (German reference surface, Normalnull NN), which is approximately 2 m above the lowest astronomical tide



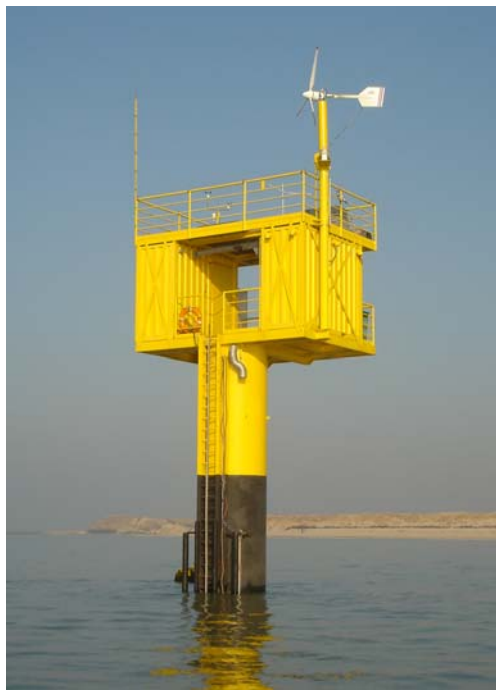


Fig. 2 View of the time-series station *Wattenmeer*

station. It also carries the antenna of a beam radio link system for data transfer to a receiving station on Spiekeroog island where the data are forwarded to the University of Oldenburg via telephone network. Moreover, meteorological sensors are installed on the upper platform together with an electric winch for profiling underwater measurements using hydrographic probes.

2.2 Energy supply, station computer and communication

The station was designed with self-contained power supply. This is achieved with a wind energy converter (AeroCraft® AC 752) and solar modules (Siemens® SM110-24) mounted on the upper platform, having a nominal output power of 750 and 110 W, respectively. The electric power is stored in 24 lead accumulators (BAE® 10 OPzV 1000, 2 V nominal cell voltage, total capacity 2,000 Ah), which are assembled in one of the containers and provide the 24 V DC operating voltage of the station. DC/DC and DC/AC converters provide 12 and ± 15 V DC and 230 V AC voltages for specific applications. In case of extended periods with low wind and daylight conditions leading to low battery voltage, a gas-fuelled power generator (2,000 W) with remotely controlled start-up serves as an emergency reserve.

The station computer (MERMAID Station Controller MSC) is an industrial PC model AT-96 iPC with an embedded DOS operating system. The software was designed to monitor the various housekeeping data and to

perform data logging of the sensors installed at the station. The MSC can work autonomously by storing the non-averaged data in a database. However, the standard mode of operation is to transmit these data via telemetry to the data bank of a laboratory-based PC at the University of Oldenburg in real-time or at pre-defined time intervals. This is realised by wireless LAN between the station and a relay receiver installed on Spiekeroog island at a distance of 4 km, where the received data are transferred to the university with ISDN telephone network. Data stored in the MSC databank are deleted following a positive response from the land-based databank (end-to-end acknowledge). These precautions for a safe data transmission along with the need for various data format changes between MSC and land-based PC limit the net data rate to approximately 10 kB/s.

The bi-directional communication between MSC and laboratory-based PC allows a remote control and servicing of instruments and sensors installed at the station. This includes, among other functions, re-boot of the MSC, control of the energy management, start and stop, and change of data sampling frequency of individual sensors. Moreover, the programmable logical controller management of the station includes an automatic shutdown of instruments and other devices of the station in case of low battery power. This is done in a sequence depending on safety relevance; the ultimately operated device is the blinker beacon installed on the upper platform.

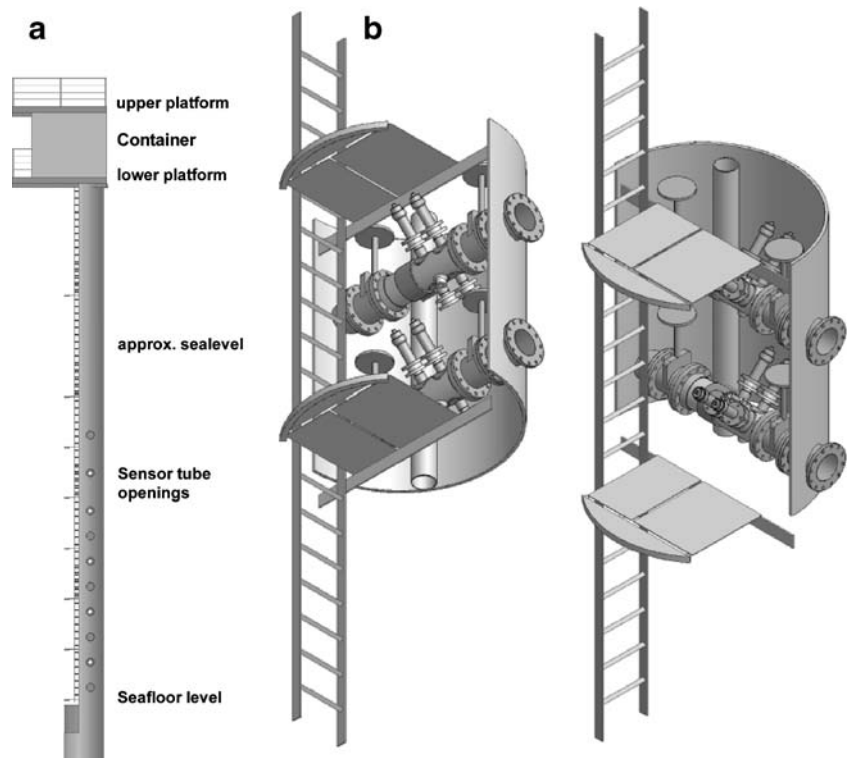
2.3 Hydrographic instruments installed inside the pole

With conventional platforms such as research vessels, oceanographic buoys and near-shore pile measurements with submersible instruments are mostly restricted to the period of spring to autumn in coastal waters of the North Sea since waves, tidal currents and ice during winter would be a high risk for the installed sensors. To overcome these limitations and to allow for a continuous data sampling also

Table 1 Dimensions and system parameters of the time-series station

Mechanical dimensions	Stand pipe: diameter 1620 mm, steel thickness 22 mm, length 35 m Platforms: 5.10 m \times 3.60 m; two containers, each 3.0 m \times 1.2 m
Electric energy	750 W wind turbine; 120 W solar panels; 2500 Ah 24 V batteries; 2 kW 230 V AC gas generator
Data management	Industrial PC
Telemetry	Point-to-point radio link to relay station on Spiekeroog island; transfer to land station with ISDN telephone network
Electric winch	Installed on upper platform; 6-conductor cable; load 400 N max

Fig. 3 **a** Schematics of the station, with a partial view into the pole with mounted access ladders and platforms. The sensor tubes in use are marked with clear openings. **b** A detailed view into the pole shows the ladder and platforms, and two sensor tubes. The vertical vent pipe in the background serves to feed fresh air to the lower part of the tube during operations inside the pole



during extreme weather conditions, sensors at the *Wattenmeer* station can also be used inside the pole under well-protected conditions.

This feature of the station has been realised by inserting a concrete sealing compound into the pole at the level of the seafloor, thus preventing water intrusions via sediment. Rigidly mounted vertical access ladders between the upper entry and the concrete sealing allow the pole to be accessed on five platforms at different depths between sea surface and bottom (Fig. 3). For integrating sensors, specific tubes were installed in the pole at various water depths with a horizontal orientation along the main tidal current direction.

This leads to a continuous flow of seawater to sensors, which can be attached through mounting flanges (Fig. 4). The sensor tubes are made of epoxy-glass resin, which resists biofouling better than steel does. Due to their low weight, the tubes are easy to handle for servicing and clean up. Cam slide valves at each end of the tubes allow the pole to be sealed against water intrusion before disassembling the setup.

Five sensor tubes were installed in the pole at different depths (Table 2). They are equipped with combined sensors for temperature (Pt100) and electrical conductivity (inductive type). The salinity S and density ρ are calculated from

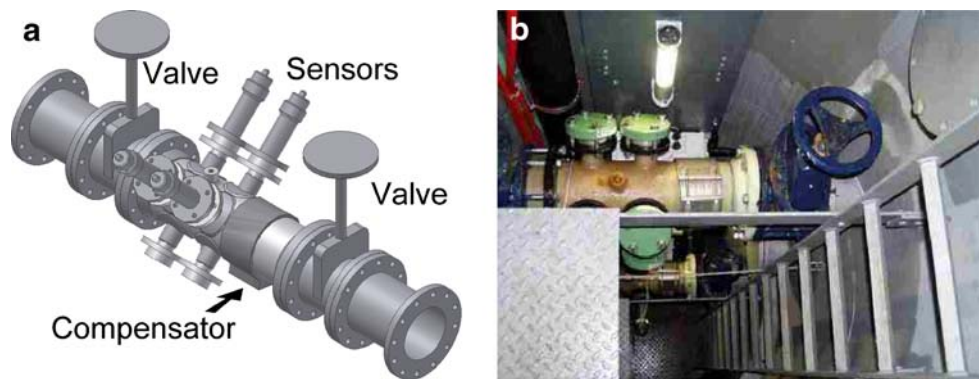


Fig. 4 **a** Schematic view of a sensor tube, with four flange-connected instruments in upward orientation. Two downward-looking flanges are shown without instruments. To avoid mechanical stress due to deformations of the pole, the sensor tube is split into two parts, which are connected by a Straub-Flex® flexible pipe coupling

(compensator), shown as a *dark ring* to the right of the sensor flanges. **b** Sensor tube mounted in the pole. A cam slide valve of the sensor tube is shown on the right in blue colour, the metallic compensator sealing the two elements of the sensor tube is shown in the *middle of the image*

Table 2 Sensor equipment installed inside the pole

Cross-over sensor tubes	At 1.5–3.5–5.5–7.5–9.0 m above seafloor (operating); at 0.5–2.5–4.5–6.5–10.5 m above seafloor (optional)
Instruments attached to sensor tubes	Temperature and conductivity (-4H- JENA engineering); Pressure (-4H- JENA engineering) at 1.5 m above seafloor
Other instruments installed in the pole	Dissolved nutrients: NH_4^+ , PO_4^{3-} , NO_2^- , $\text{NO}_2^- + \text{NO}_3^-$, $\text{Si}(\text{OH})_4$ (SYSTEA μMAC -1000 MP), inlet at 9.0 m above seafloor

temperature T , conductivity L and hydrostatic pressure p with the equations of state of seawater, i.e. $S=f(T,L,p)$ and $\rho=f(T,S,p)$ (UNESCO 1985).

The tube at 1.5 m above the seafloor carries two pressure sensors for measuring the water level, thus serving as a tide gauge. The use of an oxygen sensor (Clark cell) in the first year of operation did not yield reliable data since organisms settling on the tube surface consume oxygen, which leads to a significant decrease of oxygen concentrations during slack water. Therefore, this sensor and an additional oxygen optode sensor were later mounted outside the pole. The standard sampling rate of these sensors is one dataset every minute. More details on the sensor equipment are given in Table 2.

In late 2005, nutrient analysers (SYSTEA model μMac -1000 MP) were installed to measure the concentrations of dissolved nitrate, nitrite, ammonia, phosphate and silicate (Grunwald et al. 2007). Water samples are taken from a water inlet at the uppermost sensor tube, 9.0 m above the seafloor, and first pumped to a filtration unit equipped with a paper belt filter. The filter belt is automatically transported before each analysis cycle, its length of 100 m allowing it to be operated over more than 6 months with two filtrations per hour. The filtered water is fed to the analysers by pumps

and is then processed automatically. The measuring principle is photometrical. Reagents are stored in a refrigerator, and purified water is stored in plastic bags with a capacity that allows a 1-month operation without refill. A full nutrient measuring cycle is achieved in approximately 10 min. Measuring intervals are selectable; the standard measuring rate is one cycle per hour.

2.4 Hydrographic instruments mounted outside the pole

Several in situ instruments are operated outside the pole. These are the sensors for measuring current velocity, current direction and surface waves, light transmission, chlorophyll fluorescence and oxygen and methane concentration as well as meteorological devices. An overview is given in Table 3.

Current and surface waves are measured with an upward looking RDI model Workhorse Sentinel four-beam acoustic Doppler current profiler (ADCP; Brumley et al. 1991), which was put into operation in December 2004. Current data cannot be taken near the pole, since it strongly modifies the free flow conditions of the seawater. As a rule, a minimum distance of twice the pole diameter athwart the main current direction must be preserved to register data that are virtually unaffected. Therefore, the sensor is mounted at an 8.5 m underwater stainless steel arm extension that is fixed to the pole 2.5 m above the sea bottom and supported by five piles to provide the necessary stability. It is oriented to the northwestern margin of the main tidal channel (direction of Spiekeroog island). To avoid vibrations by current turbulence, the steel holder got additional fittings along the steel arm. The ADCP head is mounted in a free adjustable fitting at the seaward end of the steel holder, which needs a tilt-angled position to work in the wave mode. For that reason, the ADCP head is tilted 5° out of the vertical beam centre axis towards to the northern direction.

Table 3 Hydrographic and meteorological instruments outside the pole

Instruments mounted outside the pole	Acoustic Doppler current profiler (RDI Workhorse Sentinel, now: Teledyne RDI Instruments) at 1 m above seafloor Electromagnetic current sensor at 1 m above seafloor (hs engineers, model ISM-2000); Oxygen sensor, Clark type (-4H- JENA engineering) Oxygen optode sensor (Aanderaa model 3930) METS underwater methane sensor (CAPSUM, now: FRANATECH) Hyperspectral transmissometer (TriOS Optical Sensors GmbH) Chlorophyll fluorometer (Turner Designs, model SCUFA)
Meteorological sensors	Temperature (model 828), air pressure (model 8128), wind speed (model 14576), wind direction (model 14566), air humidity (model 8093.1) (Lambrecht Meteorological Instruments) Downwelling irradiance, sky and water leaving radiance (TriOS Optical Sensors GmbH, model RAMSES UV-VIS)

Operating with 1,200 kHz frequency the ADCP measures the Doppler shift and backscattering in cells (bins) of 0.2 m size, thus yielding a profile ranging from approximately 1.5 m above the seafloor to the sea surface with 0.25 m resolution. In the current mode, 45 pings are averaged over 300 s to derive a vertical profile of current velocity and direction. In the wave mode, a burst of 1,800 pings is generated with a 2 Hz ping repetition rate at intervals of 120 min, and the wave orbital velocities below the surface are measured in the cells (bins) (van Haren 2001).

Information on the amount of suspended particles can be deduced from the intensity of the backscatter signal (Hill et al. 2003), which is presently studied at the time-series station on the basis of comparisons with other methods such as particle filtration and weighing and light transmissometry.

In addition to the ADCP, an electromagnetic current metre (HS engineers, model ISM-2000) has been operated since 2004. Until 2007, the instrument was mounted on top of a pyramid-like metal frame on the seafloor at approximately 10-m distance from the pole: It measured the current velocity and direction about 1 m above the seafloor. However, this configuration did not prove to be successful, since the frame slowly sank into the sandy sediment and had to be recovered approximately every 6 months. Since 2007, the current metre is attached to the underwater steel arm close to the ADCP to provide current data just above the seafloor, i.e. at a depth below the ADCP current profile.

Attached to the pole about 0.5 m below the low tide sea level is a multispectral transmissometer (TriOS). Already planned in 2003, operation of this instrument has been hampered by strong corrosion of the probe housings made of 1.4571 stainless steel which is not seawater resistant. This was overcome with a new housing made of titanium. Qualified for use in seawater, the instrument has then been used starting in mid-2006. It measures spectra of the beam attenuation coefficient in 265 channels between the near ultraviolet and near infrared. The instrument is calibrated in situ once during workdays via telemetry using the laboratory-based PC; this feature is very useful to correct the instrument's response for biodegradation of optical windows. From the data, the specific contributions of mineral particles, gelbstoff and phytoplankton to the total attenuation spectrum can be derived with a non-linear approximation algorithm (Barth et al. 1997, 2001). Based on a comparison with standard calibration procedures, the spectral contributions from mineral particles and phytoplankton can be calibrated in mass units of suspended particulate matter and chlorophyll *a*, whereas gelbstoff is defined by its absorption coefficient at 450 nm wavelength. Combined with data from the current metres, these data serve to evaluate continuous information on material fluxes

at the position of the time-series station (Badewien et al. 2009).

In March 2007, an in situ chlorophyll fluorometer (Turner Designs, model SCUFA) was mounted opposite to the transmissometer at 0.5 m below the low tide sea level. According to recommendations by the manufacturer, its optical windows are protected against biofouling with a copper mesh, which helps to extend the servicing intervals to more than 4 weeks during the biologically productive seasons (Fig. 5a). In clear water, the dynamic range for chlorophyll detection extends from less than 0.1 to 300 $\mu\text{g/L}$. The data were calibrated against water samples taken during the spring bloom in May 2008. Chl *a* was analysed by the standard photometric method of Lorenzen (1967). A linear regression of results indicates that the SCUFA chlorophyll readings are about a factor of 4 too low, which is assumed to be caused by the loss of light intensity due to the high amount of suspended mineral particles. The corrected chlorophyll data range from approximately 1 to 35 $\mu\text{g/L}$ chl *a* during spring blooms, which are clearly visible in April/May.

Other sensors operated about 0.5 m below low tide sea level measure dissolved oxygen and methane. This cannot be done with sensors mounted in a sensor tube in the pole since oxygen and methane are strongly affected by gas producing or consuming organisms living on the inner surface of the sensor tubes. Oxygen has been measured with a Clark-type sensor (-4H- JENA engineering) since 2005 and with an Aanderaa optode model 3930 since 2006. The latter method is based on the effect of dynamic luminescence quenching (lifetime based) by molecular oxygen. Methane sensors (CAPSUM Technologie, now FRANATECH, model METS) were used in 2005–2006. The measuring principle is based on the resistance change of a semiconductor surface (SnO_2) caused by the adsorption of hydrocarbon molecules that diffuse through a silicon membrane into the detector chamber (Lamontagne et al. 2001; Garcia and Masson 2004). The time constant of the sensor is approximately 5 min, and data were sampled continuously at 10-min intervals. Measurements at the time-series station often led to unreliable data, for reasons that were not finally identified. Results obtained in 2005 are reported in Grunwald et al. (2007).

2.5 Meteorological and remote sensing instruments

A set of meteorological sensors (Lambrecht Meteorological Instruments[®]) measures air temperature and humidity, air pressure, wind speed and direction (Table 3). The sensors are attached to a pile 2 m above the upper platform, approximately 10 m above mean sea level corresponding to the standard height for wind data products.

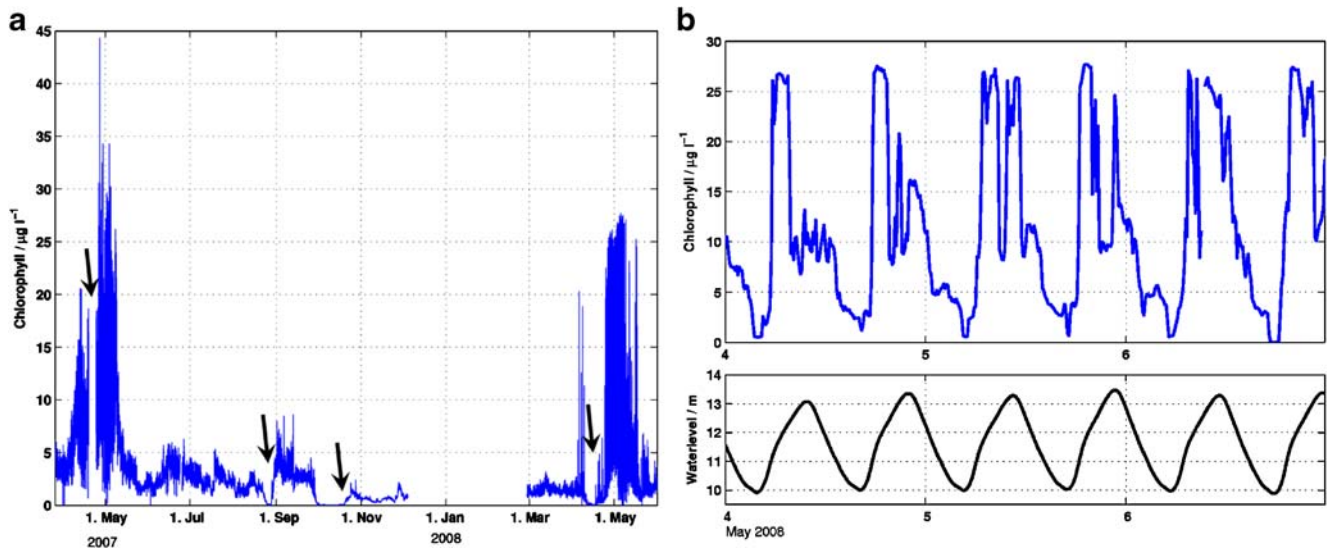


Fig. 5 **a** Time-series of chlorophyll a derived from SCUFA fluorescence readings. *Arrows* indicate times when the optical windows were cleaned, and the antifouling copper mesh was renewed. The fluorometer was not in use between December 2007 and February 2008. **b** Signals obtained during intense spring plankton blooms,

shown together with the water level for the period of 4–6 May 2008, are not noisy. During high tide, water with high phytoplankton content is transported from the open sea to the tidal flats. Concentrations are much lower during low tide, presumably caused by strong mixing of the water in the backbarrier area

Spectra of daylight illumination and of daylight reflectance from the sea surface are measured with the aim to derive data on total suspended matter in the near-surface water layer. This is done with a set of TriOS RAMSES spectroradiometers (Heuermann et al. 1999), i.e. an upward looking sensor for measuring the downwelling daylight irradiance E_d , and two sensors for measuring the upwelling radiance L_u from the water at a 30° incidence angle. The radiance sensors are oriented in an eastward direction to minimise both sun glitter from the sea surface and shadowing effects from the station. From these data, the above-water spectral reflectance

$$R_{rs}^+(\lambda) = \frac{L_u^+(\lambda)}{E_d(\lambda)}$$

is calculated. To account for contributions from light reflected by the air/water interface to the measured L_u^+ , another radiance sensor is used to measure the skylight radiance L_{sky} at a 30° zenith angle (Fig. 5). From its data, the water-leaving radiance L_u^- just beneath the sea surface and hence the so-called remote sensing reflectance $R_{rs}^-(\lambda)$ can be estimated (see, e.g. Hooker and Morel 2003).

Data are available during daylight and can be used in clear sky or homogeneous cloud conditions only. However, an advantage is the absence of biofouling of the sensors, which otherwise is a limiting factor with any optical underwater installation. Negative effects due to salt spray have not been observed, which is probably due to the installation height

above the sea surface. Examples of reflectance spectra are shown in Fig. 6b.

3 Results

3.1 Constructional layout of the station

The station has shown its value for observing extreme weather events like winter storm surges and extreme high tides. The stability of the mechanical structure remained unaffected, and instruments installed in the sensor tubes gathered data in a well-protected environment. In addition, drift ice, which occurred twice during the time of operation, was not a risk for the pile stability. The novel concept of a pole that can be internally accessed through rigidly mounted ladders and platforms did not reveal any weak points. This also holds true for the installation of crossover sensor tubes in the pole below water level with a horizontal orientation along the main tidal current direction, which allow in situ sensors to be used in a well-protected position at several depths in the water column.

The potential occurrence of a scour in the sediment around the pole had attracted much attention already in the planning phase. Although well known in principle, the processes that give rise to sediment erosion in the vicinity of such offshore constructions were unknown for the specific hydraulic environment in the tidal inlet and the

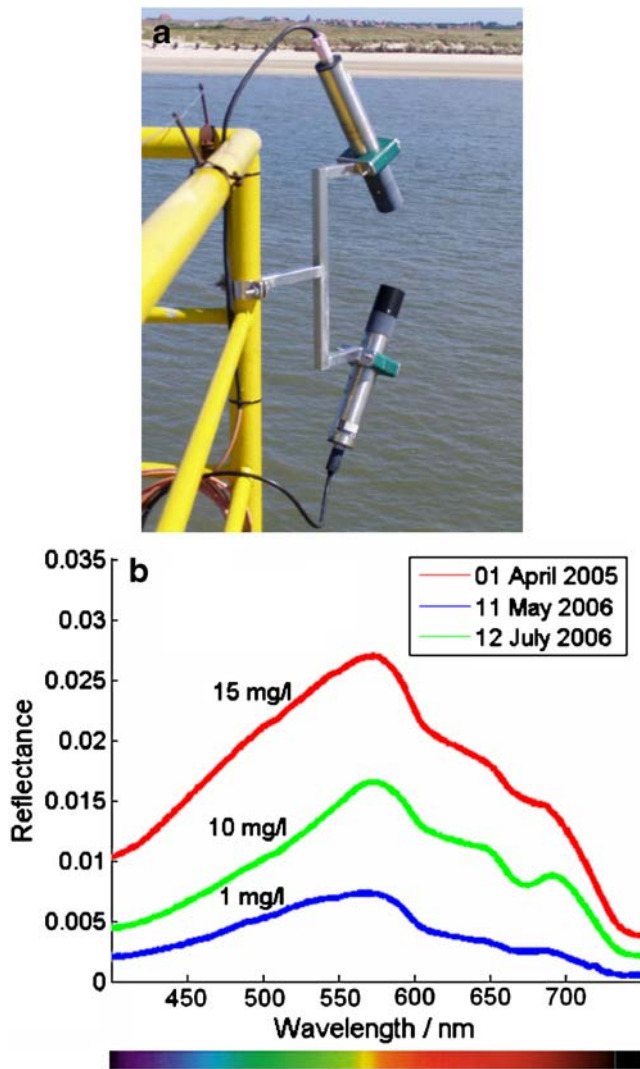


Fig. 6 **a** Radiometers mounted at the station for measuring spectral skylight radiance L_{sky} (bottom) and above-water radiance L_u (top). **b** Examples of reflectance spectra $R_{rs}^+(\lambda)$ obtained with the radiometers. Total suspended matter concentrations given as parameters to the curves were derived from data of the MERIS ocean colour instrument aboard the ESA ENVISAT satellite during overflight at the same time. The minimum at 670 nm in the green and red spectrum is due to the red absorption band of chlorophyll *a* from enhanced phytoplankton concentrations

sandy sediment at the chosen location. Driven to 10 m depth into the sediment, the pole remains stable even in case of a 1.3 m deep scour according to calculations of the manufacturer. However, already 5 months after installation, a scour that is 3 m deep was observed in a side-scan sonar survey (Fig. 7). This scour was filled with sandbags in order to keep the station's stability.

However, scours with similar dimensions occurred twice again after 2 to 3 years. They were filled with gravel in plastic bags, which were considered to provide longer term stability than the sandbags used before. Inspection by divers indicates that the scour continuously recurs since the

bags slowly sink into the sediment. Based on these observations, the hydraulic flow conditions in the tidal inlet were investigated in a detailed study in relation to characteristic features of the bedforms. It was found that scour dimensions are related to the strength of diurnal tidal currents (Normets et al. 2006), which are very intense at the position of the station, as shown in Section 3.3.

3.2 Reliability and stability of sensors and instruments

Coastal waters are often characterised by high current velocities, high suspended matter load and enhanced biological productivity. This holds true in particular for tidal flats such as the Wadden Sea. Tidal waters represent harsh conditions for all underwater instruments, which are being deployed for extended periods in time. Requirements of sensor accuracy and stability are high, but the endurance of sensors in these applications is often not well described in tables of technical characteristics given by the manufacturer.

Practical experience obtained at the time-series station provides a deeper insight into the quality and limitations of available sensors; this is summarised in Tables 4 and 5.

A strongly limiting factor for underwater sensor applications is biofouling. Besides optical instruments, electrical conductivity sensors are most problematic in terms of possible systematic errors due to growth of organisms, especially during periods of enhanced biological productivity in spring and summer (Fig. 8). Therefore, salinity data, calculated from electrical conductivity, temperature and pressure, are easily affected.

The growth of organisms on the surface of the inductive conductivity sensor typically results in a monotonic reduction of measured conductivity, and hence calculated salinity, over periods of weeks (Fig. 9). This makes a careful validation of salinity data necessary, which is done with depth profiling measurements at the station using a precisely calibrated conductivity, temperature, depth (CTD) probe (Sea-Bird model SEACAT Profiler). However, decreasing salinity data, as shown in Fig. 9 are not always an indication of sensor biofouling. Trends of the same order may result from changing freshwater run-off from land,

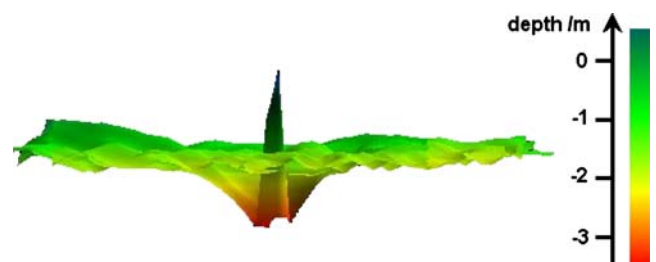


Fig. 7 Topographic image of the pile and its surrounding seabed derived from a side-scan sonar survey in February 2003, showing a 3 m deep scour

Table 4 Specifications of instruments and sensors as reported by the manufacturer and (given in italics) in use at the time-series station

Parameter	Dynamic range	Accuracy	Resolution	Stability of accuracy	Model	Manufacturer
Air temperature	-30...70°C	±0.1°C (at 0°C)	Not given		828	Lambrecht
Air pressure	600...1,100 hPa	±0.3 hPa	Not given		8128	Meteorological Instruments
Wind speed	0.7...50 m/s	±2% full scale	0.1 m/s		14576	
Wind direction	0...360°	±1%	2.5°		14566	
Air humidity	0...100%	±2% (5–95%)	Not given		8093.1	
Seawater temperature	-2...35°C	±0.035°C, 0.02°C	Not given, 0.001°C	1 year	4H Kombisonde	-4H- JENA engineering
Electrical conductivity (inductive type)	1–65 mS/cm	±0.065 mS/cm, 0.2 mS/cm ^b	Not given, 0.001 mS/cm	Nov–March: 3 months; April–Oct <2 weeks		
Underwater pressure	0–3,000 hPa	±3 hPa	Not given, 0.001 hPa	1 year		
Oxygen (Clark cell)	0–20 mg/L	±0.2 mg/L ^c	Not given	1 month		
Oxygen (Optode)	0–16 mg/L	0.3 mg/L ^d	0.03 mg/L	Nov–March: 3 months; April–Oct: 2 weeks	3930	Aanderaa
NH ₄ ⁺ , PO ₄ ³⁻	NH ₄ ⁺ : 0.01–40 μmol/L, 0.01–11 μmol/L ^a ; PO ₄ ³⁻ : 0.01–10 μmol/L, 0.01–2.1 μmol/L ^a	Not given	NH ₄ ⁺ : 0.4 μmol/L, PO ₄ ³⁻ : 0.1 μmol/L		μMAC-1000	SYSTEA
NO ₂ ⁻ , NO ₃ ⁻ + NO ₂ ⁻	NO ₂ ⁻ : 0.01–17 μmol/L, 0.01–6.5 μmol/L ^a , NO ₂ ⁻ + NO ₃ ⁻ : 0.17–60 μmol/L, 0.17–60 μmol/L ^a	Not given	NO ₂ ⁻ : 0.3 μmol/L, NO ₃ ⁻ : 1.85 μmol/L		μMAC-1000	
Si(OH) ₄	0.38–100 μmol/L, 0.38–50 μmol/L ^a	Not given	0.38 μmol/L		μMAC-1000	
Dissolved methane	0.02–10 μmol/L	0.02 μmol/L	11%		METS	CAPSUM/ FRANATECH
Multispectral transmission	Attenuation coefficient: 0.2...200 m ⁻¹	Not given, 50% ^e	Not given, 0.01 m ⁻¹	Nov–March: 3 months; April–Oct: 2 weeks	Transmissometer	TriOS Optical Sensors
Chl <i>a</i> fluorescence	0.02–20 μg/L, 1–40 μg/L	Not given, <1 μg/L	Not given 0.5 μg/L	Nov–March: 3 months; April–Oct: 2 weeks ^f	SCUFA	Turner Designs
Current profile	-5...+5 m/s	0.3%	0.1 m/s	~1 month	Workhorse Sentinel ADCP	RDI/Teledyne RDI Instruments
Current	-3...+3 m/s	1 mm/s	±1%	~1 month	ISM-2000	hs engineers

^a Grunwald et al. (2007)

^b Up to 20 mS/cm due to biofouling in periods of high biological productivity

^c Up to 80% of the true oxygen concentration due to biofouling

^d Up to 50% of the true oxygen concentration due to biofouling

^e From too high beam divergence and detector acceptance angle

^f Optional copper anti-fouling system did not show to be efficient since the mesh openings are rapidly blocked by seagrass and large particles

which often makes a correction of salinity data difficult at times of increased biological productivity.

Figure 9 exemplifies the procedure for validating salinity data. In this case, reference measurements were conducted at three points in time. In a first step, outliers were eliminated from the data set. After this, the difference between the raw and the reference data was calculated (Fig. 9b, blue dots) in order to obtain an optimised reference function (green line). This function was then used to correct the raw data. The residual differences between the validated data and the reference measurements are shown as red dots in Fig. 9b. However, if biofouling is too severe (Fig. 9a, cyan line, raw data tube 2), such a correction is inappropriate. These data are not used.

During spring and summer, when biological activity is high, calibration periods are typically a few weeks. During winter, these periods are extended up to several months.

A time series of validated data measured between January 2007 and December 2008 is shown in Fig. 10. Temperature and salinity values were taken from the best sensor mounted in the five sensor tubes, according to a comparison with the reference CTD profiles. A number of 58 reference profiles were performed, i.e. 2.3 profiles per month on average. Red dots indicate the reference temperature and salinity data; the mean deviations of data taken at the station versus reference profile are $\Delta T=0.09^{\circ}\text{C}$ and $\Delta S=0.012$ psu.

A criterion for the quality of time-series measurements is the availability of data. This has been evaluated with a focus on core parameters, which need to be measured simultaneously for an understanding of hydrographic and meteorological conditions. Core parameters include wind speed and direction, air temperature and pressure data for meteorological data and water temperature, electric conductivity and pressure for hydrographic data. Operational availability indicates that at least one meteorological or hydrographic parameter is measured. The result of this evaluation is shown in Fig. 11 and Tables 4 and 5 for the time-series station *Wattenmeer*. In 2002–2006, outliers were



Fig. 8 Inductive-type conductivity sensor (4H Kombisonde) after 3 weeks of operation in a sensor tube (photo taken on 8 Sept 2005). The blue colour is from antifouling paint. Coating of the central bore with antifouling paint is not feasible since this would affect the form factor of the sensor and hence its calibration. The bore is therefore starting point of Barnacle and Cyclops colonisation

removed from the data set, and values were checked for plausibility. In 2007–2008, only validated data are considered in the diagram.

3.3 Processes in the tidal flats

The estimation of water volume and suspended matter transport through the tidal inlet makes it necessary to measure accurate current velocity profiles. Figure 12 shows current velocities measured by the bottom-mounted

Table 5 Annual data availability in percent

Period	Meteorological availability	Hydrographic availability	Operational availability
2008	99.5	93.2	99.5
2007	94.6	97.5	99.3
2006	99.2	94.8	99.2
2005	74.8	82.0	91.3
2004	73.4	87.4	94.4
2003	18.8	53.1	69.2
2002 (Oct–Dec)	85.9	14.9	86.0
Oct 2002–Dec 2008	78.0	74.7	91.3

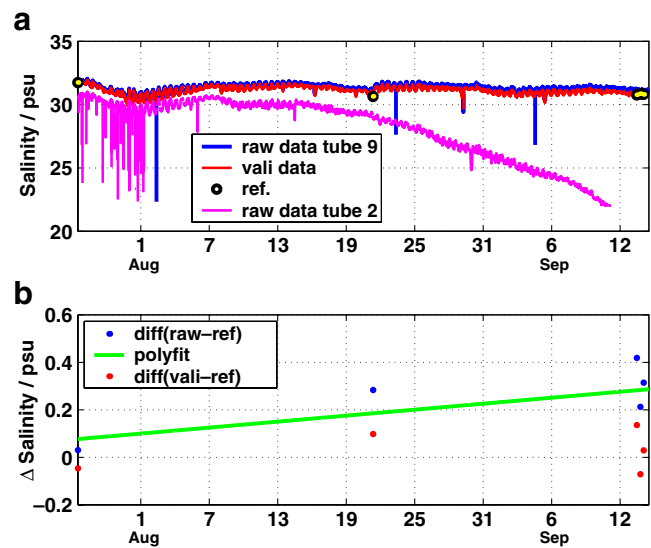
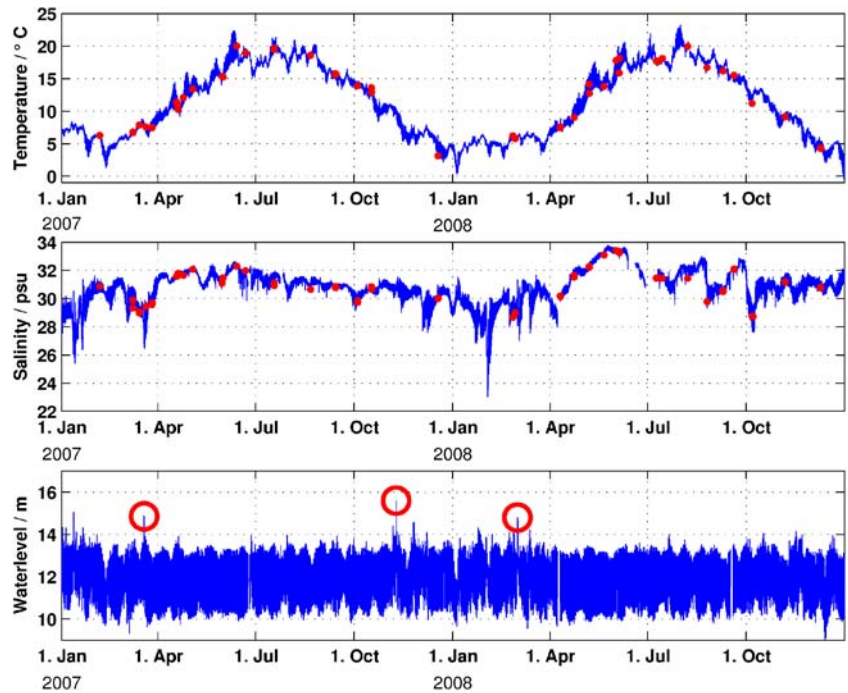


Fig. 9 a Salinity data from 24 July to 14 September 2007, calculated from temperature and conductivity measured in sensor tubes 2 and 9. Variations due to freshwater run-off can be seen in the signal of a tidal period. Increasing biofouling of the tube 2 sensor leads to an apparent decrease of salinity, which is not the case for the tube 9 sensor. SEACAT data (circles) were used as a reference, which results in the validated salinity time-series. b Salinity difference of tube 9 raw data versus reference (blue dots) and polynomial fit (green line), and remaining difference of validated tube 9 data versus reference (red dots)

Fig. 10 Time series of validated water temperature and salinity (upper and middle curves) from January 2007 to December 2008. Red dots correspond to data from reference measurements with a SeaBird SEACAT CTD probe. The water level (lower curve) taken with the pressure sensor mounted in tube 2 at 1.5 m above the seafloor shows tidal variations. Maxima marked by red circles correspond to storm tides which resulted from the storms *Orkun* (18 March 2007), *Tilo* (9 Nov 2007) and *Emma* (1 March 2008)



upward-looking ADCP. The sea surface elevation was determined concomitantly by a pressure sensor (black line in Fig. 12). Current velocities vary on timescales of days due to wind forcing and spring and neap tides. Maximum

current speeds were 1.3 m/s during inflow and 1.8 m/s during outflow. As can be derived from Fig. 12b, the slack water period during low tide is longer than during high tide. This difference is due to the station's location at the eastern side of the tidal inlet where the water passes through during ebb tide as a consequence of Coriolis deflection. In addition, this area is usually characterised as an ebb-dominated tidal system (Stanev et al. 2003a, b), leading to a tide phase asymmetry. In general, the ebb tide lasts shorter but has higher current velocities than the flood tide in an ebb-dominated system.

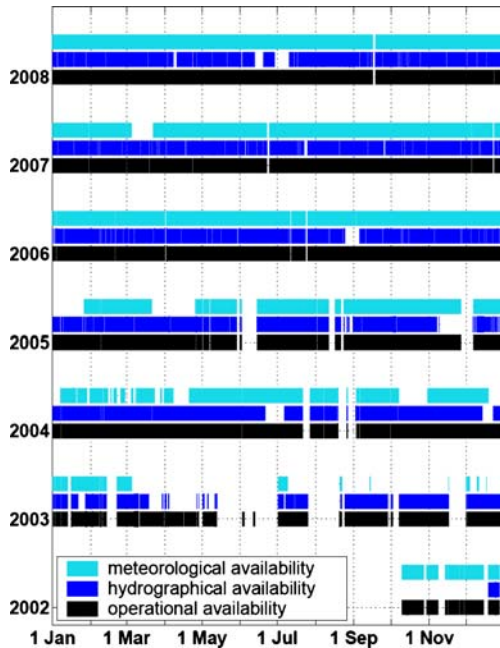


Fig. 11 Bar chart of annual data availability. Meteorological availability: wind speed and direction, air temperature and pressure data were measured simultaneously and data are available. Hydrographic availability: water temperature, electric conductivity and pressure were measured simultaneously and are available. Operational availability indicates that at least one meteorological or hydrographic parameter was measured

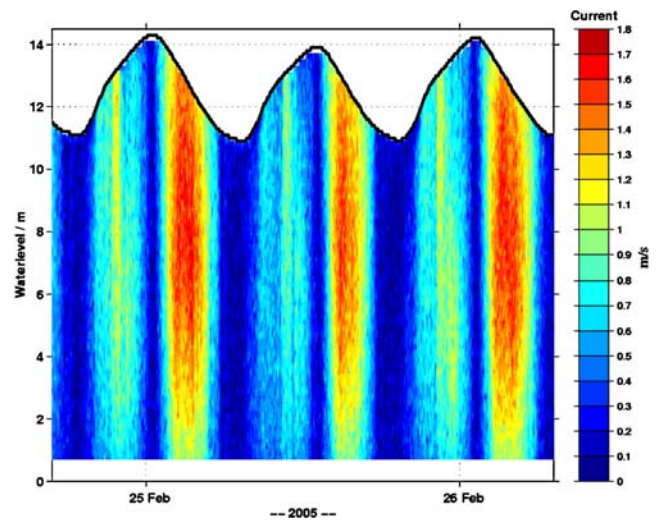


Fig. 12 Current velocity measured by a bottom-mounted upward-looking ADCP at the time series station from 24 to 26 February 2005

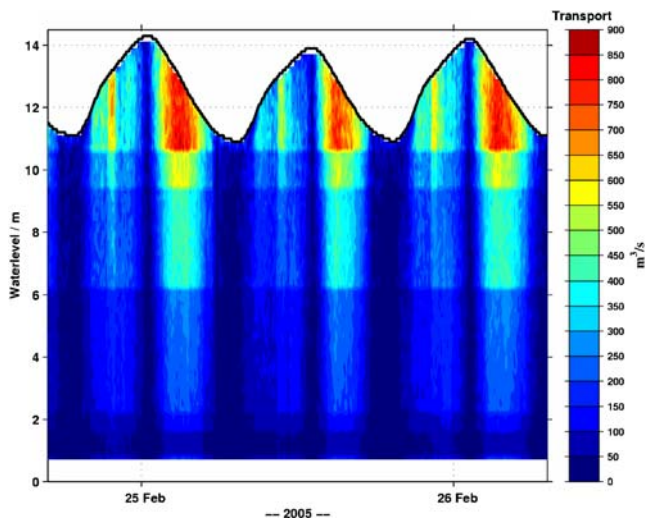
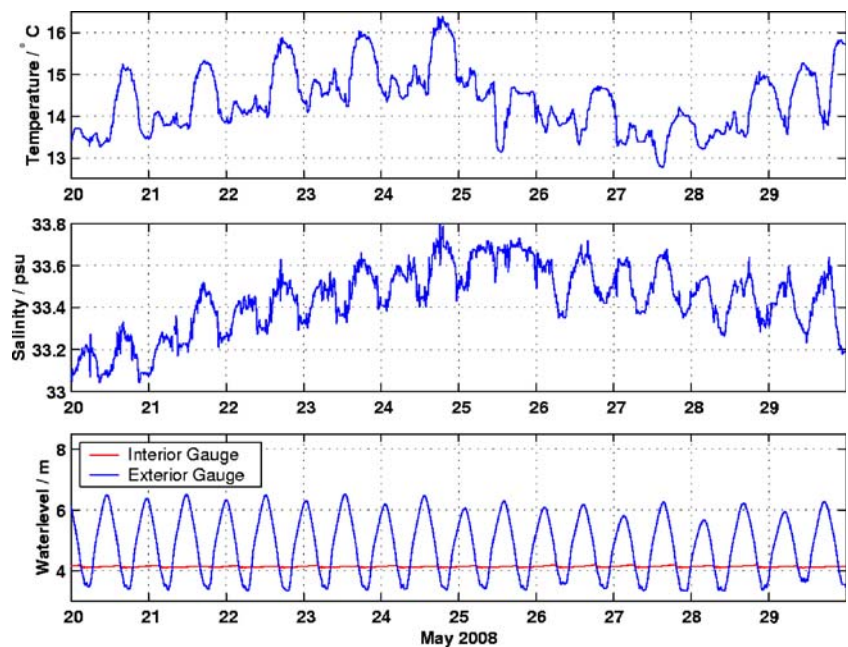


Fig. 13 Integrated volume transport through the cross-section between Spiekeroog and Langeoog islands estimated from ADCP measurements at the time series station from 24 to 26 February 2005

In order to get an idea of the volume transport through the tidal inlet, the area of the cross-section between the islands of Langeoog and Spiekeroog was estimated. This area was vertically divided into 1 m intervals, and the current velocity measured in each interval was extrapolated over the whole cross-section. The results are shown in Fig. 13: The largest part of the water volume is transported in the upper metres of the water column. It implies that — in addition to the Coriolis deflection already mentioned — measurements in the upper part of the water column are critical if transport budgets through the inlet are to be

Fig. 14 Time-series measurement of temperature and salinity measured at the time-series station, and of water level measured seawards (exterior) and landwards (interior) at the Neu-harlingersiel tide gauge from 20 to 29 May 2008. High and low water at the tide gauge is approximately 20 min later than at the station. Freshwater discharge to the harbour occurs during ebb tide, as seen by the steplike decrease of the interior water-level. This decrease is a few centimetres only, indicating the low discharge volume



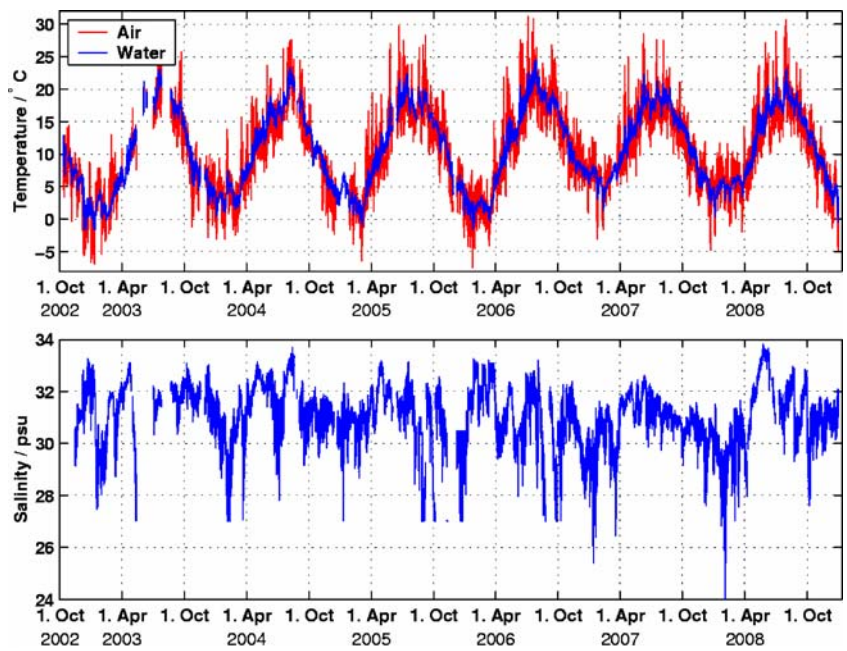
estimated. This topic will be discussed in more detail in another publication.

Another advantage of time-series measurements is the possibility of identifying exceptional hydrographic conditions in the tidal flats. An example is the evolution of salinity in May 2008 (Fig. 14).

May 2008 was characterised by very low precipitation of less than 2 mm per day in northern Germany and by more than 250 W/m² of solar radiation per day in the German Bight (Berrisford 2009). Accordingly, there was very little freshwater discharge at the tide gauge in Neuharlingersiel, as can be seen from the virtually constant water level landwards of the tide gauge in Neuharlingersiel (Fig. 14, lower graph). Temperature and salinity measured at the station increased until 25 May (Fig. 14, upper two graphs), and salinity reached high levels of about 33.7 psu, which had not been observed in other times at the time-series station (Fig. 15). The salinity maximum during low tide gives evidence of the high evaporation in the backbarrier area. Water temperature at low tide is increased by approximately 3.5°C during daylight and salinity maxima are more pronounced, which is not so during low tide at night.

A major rationale for realising the time-series station had been the expectation of measuring data also in bad weather during storms, spring tides and storm surges. Results obtained during some of these extreme events have been analysed, and they were used to validate hydrodynamic models and models of suspended matter flux. These comparisons of experimental data and model results are discussed in Lettmann et al. (2009) to which we refer.

Fig 15 Ten-min records of air and seawater temperatures (*top*) and salinity (*bottom*) from October 2002 to December 2008. No filtering has been applied to the data. Year 2007 and 2008 data are validated, outliers are removed in data from October 2002 to December 2006. Gaps in the time series are caused by malfunctions of the station computer or wireless LAN connection or by sensor failure



3.4 Multi-year time-series data

Data of air and seawater temperatures and of seawater salinity taken between October 2002 and December 2008 are shown in Fig. 15. Seasonal variations appear to be closely correlated. This seasonal covariance is caused by the strong coupling between water column and atmospheric conditions due to the very shallow water depth in the area.

The air temperature shows higher short-term fluctuations than the water temperature. Water temperatures vary also with tidal periodicity, which is a consequence of heat

exchange between air and water in the backbarrier area, leading to temperature changes of the water passing the station at ebb flow when compared to inflow conditions. This effect depends on the temperature of the inflowing coastal water, on wind, air temperature and sunlight in the tidal flats. It can thus result in higher or lower water temperatures during outflow in both summer and winter when compared to open coastal water temperatures (Figs. 16 and 17).

The salinity time series are much less dominated by seasonal factors than those of temperature. In winter, salinity values are mostly lower than those measured in summer, which is due to the higher values of precipitation minus

Fig 16 Time series of temperature, salinity and waterlevel from 7 to 14 June 2007. Water temperature at low water is higher than at high water due to warming of the seawater in the backbarrier area during high water during daylight. Salinity data are higher by approximately 0.5 psu during low water, indicating evaporation of water or low freshwater supply to the backbarrier area

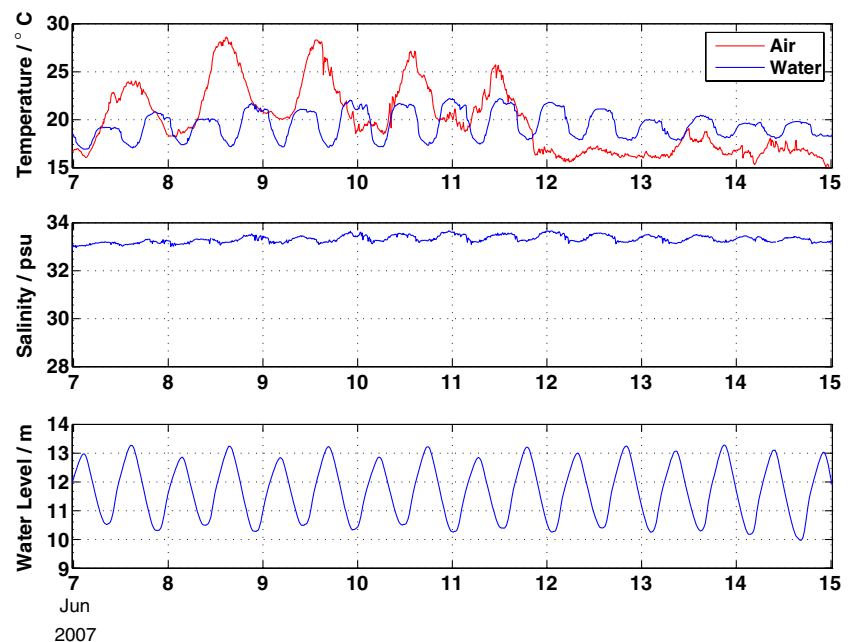
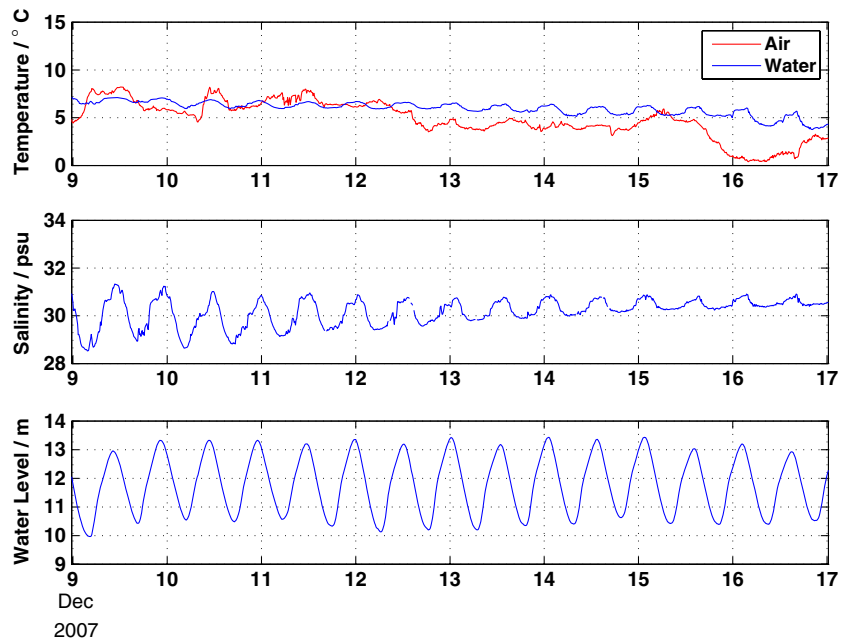


Fig 17 Time series of temperature, salinity and waterlevel from 9 to 16 December 2007. Seawater temperature variations are low and air–water temperature differences are small. Salinity shows tidal variations with minima during low water, indicating strong freshwater supply to the backbarrier area



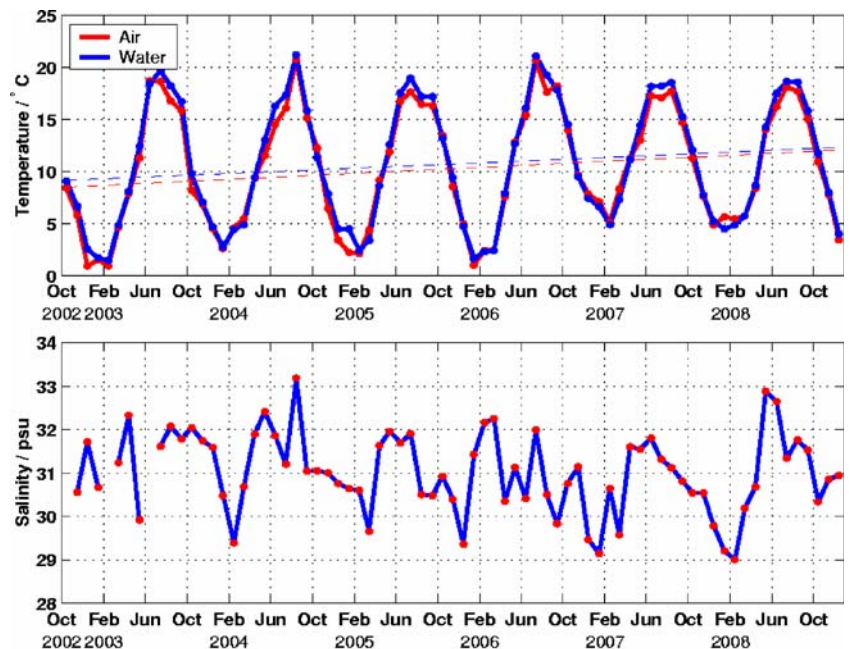
evaporation in winter and hence stronger freshwater run-off. The more frequent data gaps in the salinity diagram when compared with temperature are due to biofouling of conductivity sensors, which results in a frequent performance degradation of these sensors during periods of enhanced biological productivity, as discussed in Section 3.2.

Data of wind and air pressure show comparably much stronger short-term variations. Therefore, a graph of the full data set covering several years is not shown in this study. However, these parameters can be made available upon request in numerical form.

In order to analyse trends in the datasets of temperature and salinity, a monthly averaging was performed (Fig. 18). Again, the seasonality and the good covariance of air and water temperature are clearly seen; the correlation coefficient of air versus water temperature is 0.99. The behaviour of salinity is more irregular and uncorrelated; the correlation coefficient of water temperature versus salinity is 0.33 only.

Minimum temperature data in winter range between 1.0 and 2.6°C until winter 2005/2006 but are higher with values of about 5°C in 2006/2007 and 2007/2008. These

Fig 18 Ten-min records of air and seawater temperatures (*top*) and salinity (*bottom*) from October 2002 to December 2008 as in Fig. 15 but with a monthly averaging and best-fit line of air and water temperature (*dotted lines in the upper diagram*). Data points are plotted on the 15th day of each month



warm winters suggest a trend to rising temperatures, which has been examined by calculating a best linear fit for air and water temperature (Fig. 18, upper graph). The regression lines indicate an apparent increase of air temperature by 3.6°C and of water temperature by 3.2°C in the period from October 2002 to December 2008.

4 Discussion

The data obtained so far at the time-series station *Wattenmeer* demonstrate that the chosen location on the western side of the Spiekeroog tidal inlet is suitable for investigating the outflow of seawater and its constituents from the backbarrier tidal flats to the open German Bight. This is particularly relevant since these tidal flats correspond to an ebb-dominated tidal system. On the other hand, a more detailed knowledge of the inflowing water would be highly desirable. The comparison of experimental findings with model results shows that the characteristics of the water in the open German Bight can be modelled with good accuracy, whereas the properties of the outflow during low tide are more difficult to describe numerically. Hence, the location of the station is also suitable for the purpose of validating the results of hydrodynamic modelling (Staneva et al. 2009; Kohlmeier and Ebenhöf 2009; Burchard et al. 2008).

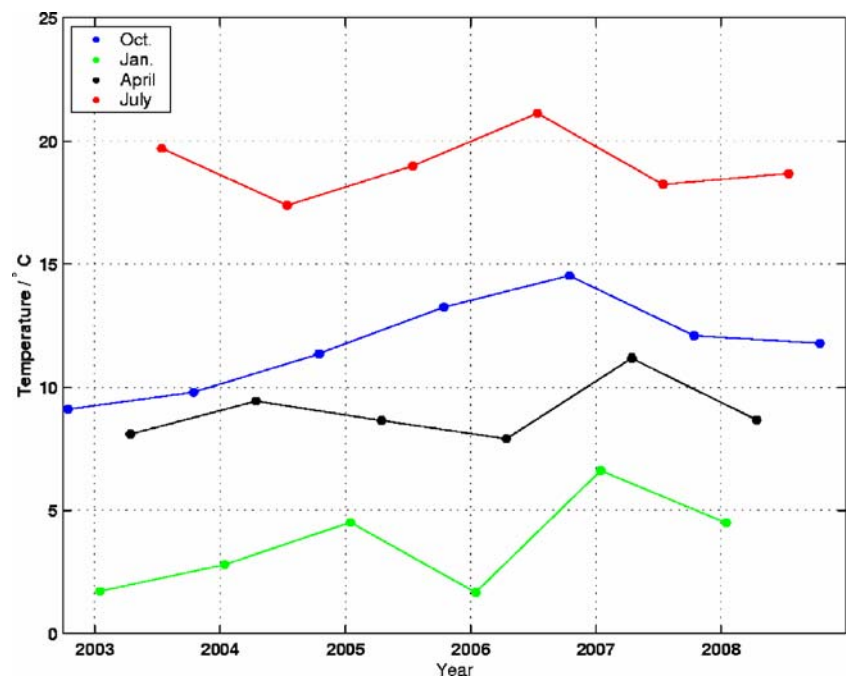
Time-series measurements offer the unique possibility to identify trends in environmental parameters, e.g. seawater temperature and salinity, which have been presented above.

It is not surprising that the seawater temperature in a very shallow coastal area such as the Wadden Sea closely follows the air temperature when viewed over time scales of months to years. Salinity is closely connected to freshwater supply and to the balance of precipitation and evaporation and is thus not much related to seasonal effects when compared with temperature.

Whereas a trend in salinity values measured from October 2002 to December 2008 is not apparent, a significant increase of approximately 3.4°C was observed in both air and seawater temperature during that period. This is essentially due to the comparably warm winters in 2006/2007 and 2007/2008. However, temperatures in winter 2008/2009 appear as low as in the winters before, and the warm winters in 2006–2008 may therefore be events not related to a secular trend. Indeed, excluding the October to December 2008 data in Fig. 18 from calculating the best fit straight lines yields an even higher temperature rise of 4.6°C in air and 4.1°C in water. This appears more correct since full years (Oct. 2002–Sept. 2008) are then used in the calculus. It shows, however, how sensitively a trend analysis depends on the chosen time period.

To examine the behaviour of water temperature at the time-series station *Wattenmeer* in more detail, representative values of four selected months are shown in Fig. 19. Obviously, the monthly data fluctuate between 3.5°C (July) and 5°C (October), and they are not monotonic over the period of observation. Therefore, assuming a linear trend of temperature rise is very doubtful. In conclusion, the present dataset cannot give evidence of a significant increase of

Fig 19 Monthly values of seawater temperature in January (green), April (black), July (red) and October (blue) in the period between October 2002 and December 2008



monthly averaged temperatures within the period of observation.

Trends of sea surface temperature in the North Sea were reported by Loewe et al. (2006). With reference to the period 1971–1993 as a climatological mean, significantly higher temperatures were found in 2002–2004, with anomalies of up to 2°C in August 2004 along the East Frisian coast. Based on the Helgoland Roads dataset, a rise of the annual mean seawater temperature of 1.33°C from 1975 to 2005 was found (Wiltshire et al. 2008). These data also provide evidence of a year-by-year variability of the annual mean temperature of typically one degree. Therefore, an identification of significant trends makes it necessary to investigate long periods in time.

5 Conclusions

After 6 years of operation, the time-series station has demonstrated its value for long-term data sampling in a challenging environment like a tidal inlet of the Wadden Sea. This refers to both the mechanical construction and the methods of measurement of hydrographic parameters.

The quality of sensor data and the procedures chosen for their validation is of utmost importance for an environmental database. Well-defined procedures have been established for the open ocean by IOC (1993) and by the World Ocean Circulation Experiment (WOCE) Hydrographic Programme for measuring procedures and accuracies (King et al. 2001) and data management (Lindstrom and Legler 2001). Generally accepted regulations do not exist for coastal waters. Techniques and methods have been drawn up for coastal zone monitoring with in situ measurements and remote sensing (Doerffer et al. 2008), with emphasis on novel methods but without specifying quality requirements. This holds true also with the Coastal Ocean Observations Module of the Global Ocean Observing System (UNESCO 2003, 2005).

For the Baltic Operational Oceanographic System, protocols and data accuracies were identified for core parameters measured at fixed stations such as temperature (0.1...0.001°C), salinity (0.01...0.001 psu) and oxygen (0.01...0.5 mg/l) and performance criteria for pre-deployment check, during deployment validation and data processing (Badewien and Krüger 2003). It can be stated that the quality of data obtained at the time-series station *Wattenmeer* is in accordance with these requirements.

Acknowledgements Numerous discussions with the team members of the research project *Biogeochemistry of Tidal Flats* were required to identify the design and functionality of the Time Series Station *Wattenmeer*. The patience of our colleagues in these meetings is gratefully appreciated. We are very much indebted to -4H- JENA engineering GmbH, Jena, Germany and in particular to Manfred

Koch, Michael Boer, Stefan Marx, Michael Kauder and Stefan Ernst for realising the time-series station. Our thanks go to Wolfram Mett, Reinhard Glissmann and Wolfgang Grefe from Ludwig Voss GmbH, Cuxhaven, for designing and building the mechanical structure of the station. Practical aspects of the station functionality were evaluated by the Wasser- und Schifffahrtsamt Emden and other authorities, which was very helpful during the construction phase of the station. We are very grateful to Ulf Harksen from the *Betriebseinheit für Technisch-Wissenschaftliche Infrastruktur*, University of Oldenburg, for his very helpful support during the construction phase. We are grateful to Olaf Jördel who designed the ADCP frame holder attached to the pole and conducted the first measurements with this set-up, to Maik Grunwald for operating the nutrient and methane analysers, to Nina Gemein for processing the RAMSES radiometer data, and to Nadine Juditzki for the phytoplankton analyses. We are also grateful to our technical staff Ingo Ötken and Bernhard Wachowicz who maintain the operation of the station very efficiently, to the captain and crew of R/V *Senckenberg* and to the technical staff of *ICBM-Terramare*, Wilhelmshaven, for their support in many campaigns to the Wadden Sea. We are also grateful to Hieronymus Meinen from Sielacht Esens for his continuous support to the project, and for making available the tide gauge data in Neuharlingersiel. The very useful comments of Reiner Oncken in his manuscript review were highly appreciated. The project is funded by the Deutsche Forschungsgemeinschaft through grants FOR 432/1-1, RE 624/5 and BR 775/14.

References

- Badewien TH, Krüger S (2003) Design of common protocols for data collection, transmission and quality control. http://www.boos.org/papa/doc/d3.2_report.doc In: PAPA Project (BOOS: Baltic Operational Oceanographic System) <http://www.boos.org/papa/>. Cited 4 Feb 2009
- Badewien TH, Zimmer E, Bartholomä A, Reuter R (2009) Towards a continuous measurement of suspended particulate matter (SPM) in turbid coastal waters. *Ocean Dynamics*. doi:10.1007/s10236-009-0183-8
- Barth H, Grisard K, Holtsch K, Reuter R, Stute U (1997) Polychromatic transmissometer for in situ measurements of suspended particles and gelbstoff in water. *Appl Optics* 36:7919–7928
- Barth H, Reuter R, Schröder M (2001) Measurement and simulation of substance specific contributions of phytoplankton, gelbstoff and mineral particles to the underwater light field in coastal waters. *EARSel eProceedings* 1(1):165–174. http://www.e proceedings.org/vol01_1/01_1_barth1.pdf (last date accessed: 04 Feb 2009)
- Berrisford P (2009) The current climate. National Centre for Atmospheric Science, UK. http://ncas-cms.nerc.ac.uk/html_umdocs/current_climate/. Diagnostics for May 2008. http://ncas-cms.nerc.ac.uk/html_umdocs/current_climate/may2008/diags.html. Cited 02 Feb 2009
- Brumley BH, Cabrera RG, Deines KL, Terray EA (1991) Performance of a broad-band acoustic Doppler current profiler. *IEEE J Oceanic Eng* 16(4):402–407
- Burchard H, Flöser G, Staneva JV, Badewien TH, Riethmüller R (2008) Impact of density gradients on net sediment transport into the Wadden Sea. *J Phys Oceanogr* 38:566–587. doi:10.1175/2007JPO3796.1
- Doerffer R, Colijn F, van Beusekom J (eds) (2008) Observing the Coastal Sea—an atlas of advanced monitoring techniques. LOICZ Reports and Studies No. 33. Geesthacht, Germany: GKSS Research Centre <http://www.loicz.org/imperia/md/>

- [content/loicz/print/rsreports/marcopoli_r_s_33.pdf](#) Cited 04 Feb 2009
- Dyer K R (ed) (2000) Nearshore and coastal oceanography. Intertidal mudflats: properties and processes. Part I: Mudflat properties. *Continental Shelf Research* 20 (10–11); Part II: Mudflat processes. *Continental Shelf Research* 20 (12–13)
- Ehlers J (1988) *The Morphodynamics of the Wadden Sea*. Balkema, Rotterdam, p 397
- Garcia ML, Masson M (2004) Environmental and geologic application of solid-state methane sensors. *Environ Geol* 46(8):1059–1063
- Grunwald M, Dellwig O, Liebezeit G, Schnetger B, Reuter R, Brumsack H-J (2007) A novel time-series station in the Wadden Sea (NW Germany): first results on continuous nutrient and methane measurements. *Mar Chem* 107:411–421
- Heuermann R, Reuter R, Willkomm R (1999) RAMSES: A modular multispectral radiometer for light measurements in the UV and VIS. *Environmental Sensing and Applications. Proc. EUROPTO Series. SPIE* 3821:279–285
- Hill DC, Jones SE, Prandle D (2003) Derivation of sediment resuspension rates from acoustic backscatter time-series in tidal waters. *Cont Shelf Res* 23:19–40
- Hooker SB, Morel A (2003) Platform and environmental effects on above-water determinations of water-leaving radiances. *J Atmos Ocean Technol* 20:187–205
- IOC Manuals and Guides No. 26 (1993) Manual of quality control procedures for validation of oceanographic data. Intergovernmental Oceanographic Commission (IOC/UNESCO), Paris, France, 437 pp. http://ioc-unesco.org/index.php?option=com_oe&task=viewDocumentRecord&docID=874. Cited 04 Feb 2009
- King B A, Firing E, Joyce TM (2001) Shipboard observations during WOCE, chapter 3.1. In: Siedler G, Church J, Gould J (eds) *Ocean circulation & climate*. *Int Geophys Ser* 77:99–122
- Kohlmeier C, Ebenhöf W (2009) The challenge of modelling the biogeochemical processes of a tidal ecosystem. *Ocean Dynamics*. doi:10.1007/s10236-009-0188-3
- Lamontagne R A, Rose-Pehrsson SL, Grabowski K E, Knies D L (2001) Response of METS sensor to methane concentrations found on the Texas–Louisiana shelf in the Gulf of Mexico. *Naval Research Laboratory Memorandum Report* 6110-01-8584
- Lettmann K, Wolff J-O, Badewien T (2009) Impact of wind generated surface gravity waves and storm surges on sediment dynamics of an intertidal flat system in the East Frisian Wadden Sea (Southern North Sea, Germany). *Ocean Dynamics*. doi:10.1007/s10236-009-0194-5
- Lindstrom E J, Legler D M (2001) Developing the WOCE global data system, chapter 3.5. In: Siedler G, Church J, Gould J (eds) *Ocean circulation & climate*. *Int Geophys Ser* 77:181–191
- Loewe P, Becker B, Brockmann U, Dick S, Frohse A, Herrmann J, Klein B, Klein H, Nies H, Schmolke S, Schrader D, Schulz A, Theobald N, Weigelt S (2006) Nordseezustand 2004. Bericht 40, Bundesamt für Seeschifffahrt und Hydrographie, Hamburg, Germany (224 pp). <http://www.bsh.de/de/Produkte/Buecher/Berichte/Bericht40/BSH-Bericht40.pdf>. Cited 04 Feb 2009
- Lorenzen CJ (1967) Determination of chlorophyll and pheopigments: spectrophotometric equations. *Limnol Oceanogr* 12:343–346
- Normets R, Ernstsens VB, Bartholomä A, Flemming BW, Hebbeln D (2006) Implications of bedform dimensions for the prediction of local scour in tidal inlets: a case study from the southern North Sea. *Geo-Mar Lett* 26:165–176
- Postma H (1982) *Hydrography of the Wadden Sea: movements and properties of water and particulate matter*. Final report on ‘Hydrography’ of the Wadden Sea Working Group. In: Wolff WJ (ed) *Ecology of the Wadden Sea*. Balkema, Rotterdam, 2/1–2/75
- Reise K (1985) *Tidal flat ecology. An experimental approach to species interactions*. Springer, Berlin, p 191
- Stanev EV, Wolff J-O, Burchard H, Bolding K, Flöser G (2003a) On the circulation in the East Frisian Wadden Sea: Numerical modelling and data analysis. *Ocean Dynamics* 53:27–51
- Stanev EV, Flöser G, Wolff J-O (2003b) Dynamical control on water exchanges between tidal basins and the open ocean. A case study for the East Frisian Wadden Sea. *Ocean Dynamics* 53:146–165
- Staneva J, Stanev E, Wolff J-O, Badewien TH, Reuter R, Flemming B, Bartholomä A, Bolding K (2009) Dynamics and sediment dynamics in the German Bight. A focus on observations and numerical modelling in the East Frisian Wadden Sea. *Cont Shelf Res* 29(1):302–319
- UNESCO (1985). *The international system of units (SI) in oceanography*. *Technical Papers in Marine Science* 45, 124 pp
- UNESCO (2003) *The integrated strategic design plan for the coastal ocean observations module of the global ocean observing system*. GOOS Report No. 125, 190 pp. http://www.ioc-goos.org/index.php?option=com_oe&task=viewDocumentRecord&docID=105. Cited 04 Feb 2009
- UNESCO (2005) *An implementation strategy for the coastal module of the global ocean observing system*. GOOS Report No. 148, 141 pp. http://www.ioc-goos.org/index.php?option=com_oe&task=viewDocumentRecord&docID=127. Cited 04 Feb 2009
- Van Haren H (2001) Estimates of sea level, waves and winds from a bottom-mounted ADCP in a shelf sea. *J Sea Res* 45:1–14
- Wiltshire KH, Malzahn AM, Wirtz K, Greve W, Janisch S, Mangelsdorf P, Manly BFJ, Boersma M (2008) Resilience of North Sea phytoplankton spring bloom dynamics: an analysis of long-term data at Helgoland Roads. *Limnol Oceanogr* 53 (4):1294–1302